Journal of Theoretical and Applied Physics (2020) 14:121–128
https://doi.org/10.1007/s40094-020-00369-2

RESEARCH

# Behaviour of sheath in electronegative warm plasma

**Rajat Dhawan[1] · Hitendra K. Malik[1]**

Received: 2 January 2020 / Accepted: 8 February 2020 / Published online: 17 February 2020


**Abstract**

Behaviour of sheath formed on two types of probes, namely cylindrical and spherical probes, has been investigated in terms of its thickness, in front of the conducting probes immersed in an electronegative plasma for different negative to positive ion mass ratios, by considering three electronegative gases, i.e. $CF_4$, $O_2$ and $C_{60}$. Contrary to others' work, complete fluid equations are written for negative ions also in addition to those of positive ions considering their different masses. Increasing negative to positive ion mass ratio is found to result in an increment of the sheath thickness. The magnitude of the sheath thickness is enhanced with an increment in the positive ions' temperature, whereas the magnitude of the sheath thickness is reduced with increased negative ions' temperature and background density of the negative ions. The analysis of the case of a large probe radius, used in the surface-nitriding process, for both the geometries is attended. Additionally, the comparison between the results for electropositive plasma and electronegative plasma and for behaviour of negative ions with their Boltzmann distribution and fluid approach has also been attempted herewith and a noteworthy difference is realized. The case of doubly charged ions is also entertained herewith.

**Keywords** Electronegative plasma · Mass ratio · Sheath thickness · Ion temperature · Doubly charged ions

## Introduction

Electronegative plasmas are of enormous interest due to their expanding applications in many fields, like deposition of thin films [1–4], sterilization process [5], plasma–surface interaction [6–10], semiconductor industries [11], microelectronics industries [12], etc., where plasma containing both positive and negative ions is preferable. In many applications, they serve as ion source because of the requirement of both positive and negative ion beams; these have also been used in low-energy beam applications and also when energetic electrons can produce destructive effects on the surface [13]. Therefore, the temperature of the ions deposited on the surface of the material under investigation is essential to take care of, as it can lead to significant changes in the surface properties. The best method to ward off irregular shapes is the addition of negative ions to counterbalance the positive ions, assemble on the wafer and also to enhance the working of materials using in the fabrication of integrated circuits. Electronegative plasmas are widely adopted for soft substrates to have a defect-free analysis, as they develop immensely small sheath voltage in comparison with electropositive one.

The immersion of a metallic probe in a plasma containing electrons, positive ions and negative ions results in a non-neutrality region surrounding it, termed as the sheath. The theoretical study of the sheath formation is useful in surface hardening process like plasma immersion ion implantation [14], in mass spectroscopy [15] where analysis of the formation of the sheath at spectrometer entrance window is required for the correct interpretations of the results. Probe analysis permits us to measure the useful quantities like potential profile, density distributions of plasma species, electric field profile, sheath thickness, etc. On the other hand, by characterizing the dust grain as a conducting spherical probe in plasma, one can determine the potential with the help of probe theories [16, 17]. The usefulness of probe theories also lies in the inspection of the nature of plasma surrounding a satellite in outer space. Many authors have observed the noteworthy influence on the characteristics of the probe in the cases of low-frequency sheath processes [18–20]. Also, X-ray emission has been observed

✉ Hitendra K. Malik
hitendra.k.malik@gmail.com

1 Plasma Science and Technology Laboratory, Department of Physics, Indian Institute of Technology Delhi, New Delhi 110016, India

when laser light is launched on tin slab forming a sheath of ions which radiate [21–23].

Due to the presence of second negative species, i.e. negative ions, the plasma parameters are of a distinctive nature [24, 25]. In this paper, we deal with three electronegative gases: one which contains halogen, i.e. fluorocarbon ($CF_4$) [26], and other two gases, those do not contain halogen, are oxygen plasma [27] and $C_{60}$ plasma [28, 29]. Such electronegative gases are adopted because of their ability to produce high negative ion density compared to that of the electrons. The difference between the mobilities of two types of the ions is not high, so these must be examined by similar treatment as opposed to the others' work [30–35] where Maxwellian approximation (Boltzmann distribution) is considered for negative ions and the mass of negative ions is neglected. The negative ions also should be described by the fluid equations as in the case of positive ions to study a realistic situation. Unlike others, we also consider the drift term in the momentum transfer equation of negative ions to explore the practical case by taking into account the generalized situation of their different masses from the positive ions. In the present work, we investigate the sheath thickness profile as a function of the temperatures of positive and negative ions, electronegativity and negative to positive ion mass ratios. The studies are conducted for two cylindrical and spherical geometries, i.e. when cylindrical and spherical probes are immersed in the plasma and sheath is formed on them. A comparative study of the sheath thickness profile for the negative ions' behaviour by Boltzmann distribution and fluid approach is also entertained herewith to validate the choice of fluid approach for negative ions also.

## Basic equations

To reveal the sheath structure formed surrounding the cylindrical and spherical probes, we consider a collision-less, unmagnetized and warm electronegative plasma, where the continuity and momentum transfer equations describe the behaviour of positive and negative ions. Poisson's equation reveals the dependency of a potential profile on various factors, like temperature, mass ratio, density, etc. These equations are written as follows:

$$\frac{1}{r^K}\frac{\mathrm{d}}{\mathrm{d}r}\left(r^K n_\mathrm{P} v_\mathrm{P}\right) = 0, \tag{1a}$$

$$\frac{1}{r^K}\frac{\mathrm{d}}{\mathrm{d}r}\left(r^K n_\mathrm{N} v_\mathrm{N}\right) = 0, \tag{1b}$$

$$M_\mathrm{P} v_\mathrm{P} n_\mathrm{P}\frac{\mathrm{d}v_\mathrm{P}}{\mathrm{d}r} = Z_\mathrm{P} n_\mathrm{P} e\vec{E} - \vec{\nabla} P_\mathrm{P}, \tag{2a}$$

$$M_\mathrm{N} v_\mathrm{N} n_\mathrm{N}\frac{\mathrm{d}v_\mathrm{N}}{\mathrm{d}r} = -Z_\mathrm{N} n_\mathrm{N} e\vec{E} - \vec{\nabla} P_\mathrm{N}, \tag{2b}$$

$$\frac{\mathrm{d}^2\varphi}{\mathrm{d}r^2} + \frac{K}{r}\frac{\mathrm{d}\varphi}{\mathrm{d}r} = -\frac{e}{\varepsilon_0}\left(Z_\mathrm{P} n_\mathrm{P} - Z_\mathrm{N} n_\mathrm{N} - n_\mathrm{e}\right). \tag{3}$$

We consider that the behaviour of electrons is governed by their usual Boltzmann distribution. Hence,

$$n_\mathrm{e} = n_{\mathrm{e}0}\exp\left(\frac{e\varphi}{k_\mathrm{B} T_\mathrm{e}}\right) \tag{4}$$

In these equations, $M_\mathrm{P}$ and $M_\mathrm{N}$ are masses, $v_\mathrm{P}$ and $v_\mathrm{N}$ are velocities, $n_\mathrm{P}$ and $n_\mathrm{N}$ are densities, and $Z_\mathrm{P}$ and $Z_\mathrm{N}$ are charges of positive and negative ions, respectively. $K$ designates the geometry of probe, with values 1 and 2 for the cylindrical and spherical geometries, respectively. $n_{\mathrm{e}0}$ is the background electron density in plasma. $\varphi$ is the electric potential, which is a function of distance $r$ from the position of the probe. With respect to plasma, the probe is considered to be at the negative potential. $P_\mathrm{P}$ and $P_\mathrm{N}$ are the pressure gradient terms for positive and negative ions, respectively, defined as:

$$P_\mathrm{P} = \frac{K_\mathrm{B}\gamma_\mathrm{P}}{n_{\mathrm{P}0}^{C-1}} n_\mathrm{P}^C, \tag{5a}$$

$$P_\mathrm{N} = \frac{K_\mathrm{B}\gamma_\mathrm{N}}{n_{\mathrm{N}0}^{C-1}} n_\mathrm{N}^C. \tag{5b}$$

where $\gamma_\mathrm{P}$ and $\gamma_\mathrm{N}$ are the temperatures, and $n_{\mathrm{P}0}$ and $n_{\mathrm{N}0}$ are the background densities of positive and negative ions, respectively. $C$ is polytropic constant with value 3 for large probe radius for both the geometries.

When these results are introduced in Eqs. (2a) and (2b), the resulting equations appear as:

$$M_\mathrm{P} v_\mathrm{P}\frac{\mathrm{d}v_\mathrm{P}}{\mathrm{d}r} + Z_\mathrm{P} e\frac{\mathrm{d}\varphi}{\mathrm{d}r} + \frac{CK_\mathrm{B}\gamma_\mathrm{P} n_\mathrm{P}^{C-2}}{n_{\mathrm{P}0}^{C-1}}\frac{\mathrm{d}n_\mathrm{P}}{\mathrm{d}r} = 0, \tag{6a}$$

$$M_\mathrm{N} v_\mathrm{N}\frac{\mathrm{d}v_\mathrm{N}}{\mathrm{d}r} - Z_\mathrm{N} e\frac{\mathrm{d}\varphi}{\mathrm{d}r} + \frac{CK_\mathrm{B}\gamma_\mathrm{N} n_\mathrm{N}^{C-2}}{n_{\mathrm{N}0}^{C-1}}\frac{\mathrm{d}n_\mathrm{N}}{\mathrm{d}r} = 0. \tag{6b}$$

Quasi-neutrality condition is stated as follows:

$$Z_\mathrm{P} n_{\mathrm{P}0} \cong Z_\mathrm{N} n_{\mathrm{N}0} + n_{\mathrm{e}0} \tag{7}$$

To carry out the equations in dimensionless form, we normalized them with suitable normalization parameters, defined as follows:

$$x = \frac{r}{\lambda_{\mathrm{d}}}, y = -\frac{e\varphi}{k_{\mathrm{B}}T_{\mathrm{e}}}, N_{\mathrm{P}} = \frac{n_{\mathrm{P}}}{n_{\mathrm{e0}}}, N_{\mathrm{N}} = \frac{n_{\mathrm{N}}}{n_{\mathrm{e0}}},$$
$$N_{\mathrm{e}} = \frac{n_{\mathrm{e}}}{n_{\mathrm{e0}}}, \chi_{\mathrm{P}} = \left(\frac{v_{\mathrm{P}}}{v_{\mathrm{P0}}}\right)^2, \chi_{\mathrm{N}} = \left(\frac{v_{\mathrm{N}}}{v_{\mathrm{P0}}}\right)^2.$$

where $v_{\mathrm{P0}}$ and $\lambda_{\mathrm{d}}$ are, respectively, the ion-acoustic speed and Debye length, described as:

$$\lambda_{\mathrm{d}} = \sqrt{\frac{\varepsilon_0 K_{\mathrm{B}} T_{\mathrm{e}}}{n_{\mathrm{e0}} e^2}}, v_{\mathrm{P0}} = \sqrt{\frac{2K_{\mathrm{B}}T_{\mathrm{e}}}{M_{\mathrm{P}}}}.$$

After normalization, the above equations will appear as:

$$\frac{1}{x^K}\frac{\mathrm{d}}{\mathrm{d}x}\left(x^K N_{\mathrm{P}} \chi_{\mathrm{P}}^{\frac{1}{2}}\right) = 0, \tag{8a}$$

$$\frac{1}{x^K}\frac{\mathrm{d}}{\mathrm{d}x}\left(x^K N_N \chi_{\mathrm{N}}^{\frac{1}{2}}\right) = 0, \tag{8b}$$

$$2\sqrt{\chi_{\mathrm{P}}}\frac{\mathrm{d}}{\mathrm{d}x}\sqrt{\chi_{\mathrm{P}}} - Z_{\mathrm{P}}\frac{\mathrm{d}y}{\mathrm{d}x} + \frac{CT_{\mathrm{P}}N_{\mathrm{P}}^{C-2}}{N_{\mathrm{P0}}^{C-1}}\frac{\mathrm{d}N_{\mathrm{P}}}{\mathrm{d}x} = 0, \tag{9a}$$

$$2\frac{M_{\mathrm{N}}}{M_{\mathrm{P}}}\sqrt{\chi_{\mathrm{N}}}\frac{\mathrm{d}}{\mathrm{d}x}\sqrt{\chi_{\mathrm{N}}} + Z_{\mathrm{N}}\frac{\mathrm{d}y}{\mathrm{d}x} + \frac{CT_{\mathrm{N}}N_{\mathrm{N}}^{C-2}}{N_{\mathrm{N0}}^{C-1}}\frac{\mathrm{d}N_{\mathrm{N}}}{\mathrm{d}x} = 0, \tag{9b}$$

$$\frac{\mathrm{d}^2 y}{\mathrm{d}x^2} + \frac{K}{x}\frac{\mathrm{d}y}{\mathrm{d}x} = \left(Z_{\mathrm{P}}N_{\mathrm{P}} - Z_{\mathrm{N}}N_{\mathrm{N}} - N_{\mathrm{e}}\right), \tag{10}$$

$$N_{\mathrm{e}} = \exp(-y), \tag{11}$$

$$Z_{\mathrm{P}}N_{\mathrm{P0}} = Z_{\mathrm{N}}N_{\mathrm{N0}} + N_{\mathrm{e0}}. \tag{12}$$

Here, we defined $T_{\mathrm{P}} = \frac{\gamma_{\mathrm{P}}}{T_{\mathrm{e}}}$ and $T_{\mathrm{N}} = \frac{\gamma_{\mathrm{N}}}{T_{\mathrm{e}}}$ as the temperature ratio of the positive ions and negative ions, respectively, to electrons. $N_{\mathrm{P0}} = \frac{n_{\mathrm{P0}}}{n_{\mathrm{e0}}}$ and $N_{\mathrm{N0}} = \frac{n_{\mathrm{N0}}}{n_{\mathrm{e0}}}$ are defined as background density ratios of the positive ions and negative ions, respectively, to the electrons. $N_{\mathrm{P0}}$ and $N_{\mathrm{N0}}$ are, respectively, designated as electropositivity and electronegativity of the plasma.

Normalized positive and negative ion current ($i_{\mathrm{P}}$ and $i_{\mathrm{N}}$) collected at the probe surface can be described as:

$$i_{\mathrm{P}} = \frac{I_{\mathrm{P}}}{x_{\mathrm{P}}^{2-K}} = \frac{Z_{\mathrm{P}}N_{\mathrm{P}}\sqrt{\chi_{\mathrm{P}}}x^K}{x_{\mathrm{P}}^{2-K}} \tag{13a}$$

$$i_{\mathrm{N}} = \frac{I_{\mathrm{N}}}{x_{\mathrm{P}}^{2-K}} = -\frac{Z_{\mathrm{N}}N_{\mathrm{N}}\sqrt{\chi_{\mathrm{N}}}x^K}{x_{\mathrm{P}}^{2-K}} \tag{13b}$$

Here, $x_{\mathrm{P}}$ corresponds to the probe radii. Integrating Eqs. (8a) to (9b) and using quasi-neutrality condition at the plasma, we will get:

$$x^K N_{\mathrm{P}} \chi_{\mathrm{P}}^{\frac{1}{2}} = \text{constant} = \frac{i_{\mathrm{P}}}{Z_{\mathrm{P}}} \tag{14a}$$

$$x^K N_{\mathrm{N}} \chi_{\mathrm{N}}^{\frac{1}{2}} = \text{constant} = -\frac{i_{\mathrm{N}}}{Z_{\mathrm{N}}} \tag{14b}$$

$$\frac{C\gamma_{\mathrm{P}}}{C-1}\left(\frac{Z_{\mathrm{P}}}{1+Z_{\mathrm{N}}N_{\mathrm{N0}}}\right)^{C-1} N_{\mathrm{P}}^{C+1} - \left(Z_{\mathrm{P}}y + \frac{CT_{\mathrm{P}}}{C-1}\right)N_{\mathrm{P}}^2 + \frac{i_{\mathrm{P}}^2}{x^{2K}Z_{\mathrm{P}}^2} = 0 \tag{15a}$$

$$\frac{C\gamma_{\mathrm{N}}}{C-1}\left(\frac{1}{N_{\mathrm{N0}}}\right)^{C-1} N_{\mathrm{N}}^{C+1} + \left(Z_{\mathrm{N}}y - \frac{CT_{\mathrm{N}}}{C-1}\right)N_{\mathrm{N}}^2 + \frac{M_{\mathrm{N}}}{M_{\mathrm{P}}}\frac{i_{\mathrm{N}}^2}{x^{2K}Z_{\mathrm{N}}^2} = 0 \tag{15b}$$

On solving Eqs. (15a) and (15b), the density profiles of positive and negative ions, respectively, will be obtained for appropriate parameters. For $C=3$, Eqs. (15a) and (15b) turn out to be

$$a_{\mathrm{P}}N_{\mathrm{P}}^4 - b_{\mathrm{P}}N_{\mathrm{P}}^2 + c_{\mathrm{P}} = 0 \tag{15a$'$}$$

$$a_{\mathrm{N}}N_{\mathrm{N}}^4 + b_{\mathrm{N}}N_{\mathrm{N}}^2 + c_{\mathrm{N}} = 0 \tag{15b$'$}$$

where $a_{\mathrm{P}} = \frac{3T_{\mathrm{P}}}{2}\left(\frac{Z_{\mathrm{P}}}{1+Z_{\mathrm{N}}N_{\mathrm{N0}}}\right)^2$, $b_{\mathrm{P}} = \left(Z_{\mathrm{P}}y + \frac{3T_{\mathrm{P}}}{2}\right)$, $c_{\mathrm{P}}\frac{i_{\mathrm{P}}^2}{x^{2K}Z_{\mathrm{P}}^2}$, $a_{\mathrm{N}} = \frac{3T_{\mathrm{N}}}{2}\left(\frac{1}{N_{\mathrm{N0}}}\right)^2$, $b_{\mathrm{N}} = \left(Z_{\mathrm{N}}y - \frac{3T_{\mathrm{N}}}{2}\right)$ and $c_{\mathrm{N}} = \frac{M_{\mathrm{N}}}{M_{\mathrm{P}}}\frac{i_{\mathrm{N}}^2}{x^{2K}Z_{\mathrm{N}}^2}$.

Solutions of Eqs. (15a$'$) and (15b$'$) are obtained as:

$$N_{\mathrm{P}} = \pm\sqrt{\frac{b_{\mathrm{P}} \pm \sqrt{b_{\mathrm{P}}^2 - 4a_{\mathrm{P}}c_{\mathrm{P}}}}{2a_{\mathrm{P}}}}, N_{\mathrm{N}} = \pm\sqrt{\frac{-b_{\mathrm{N}} \pm \sqrt{b_{\mathrm{N}}^2 - 4a_{\mathrm{N}}c_{\mathrm{N}}}}{2a_{\mathrm{N}}}}$$

For $C=3$, i.e. for large probe radius, these equations have four roots: two positive and two negative. Later roots are neglected, as the charged particle density cannot be negative, whereas, from positive roots, one which gives higher charge density at the sheath edge is adopted to have a significant number of ions to form the sheath and is given as follows:

$$N_{\mathrm{P}} = \sqrt{\frac{b_{\mathrm{P}} + \sqrt{b_{\mathrm{P}}^2 - 4a_{\mathrm{P}}c_{\mathrm{P}}}}{2a_{\mathrm{P}}}}, N_{\mathrm{N}} = \sqrt{\frac{-b_{\mathrm{N}} + \sqrt{b_{\mathrm{N}}^2 - 4a_{\mathrm{N}}c_{\mathrm{N}}}}{2a_{\mathrm{N}}}} \tag{16}$$

After substituting the charge particle density value in Eq. (10), one can examine the behaviour of potential surrounding the probe for different parameters like temperature, density, mass ratio, etc. The term mass ratio is appearing in Eq. (15b), in turn, will appear in the final solution of Poisson's equation and reports its dependency on various parameters and consequently will modify the behaviour significantly. Using Eqs. (11) and (16), the final form of the Poisson's equation appears as:

$$\frac{d^2y}{dx^2}+\frac{K}{x}\frac{dy}{dx}=\left(Z_P\sqrt{\frac{b_P+\sqrt{b_P^2-4a_Pc_P}}{2a_P}}-Z_N\sqrt{\frac{-b_N+\sqrt{b_N^2-4a_Nc_N}}{2a_N}}-\exp(-y)\right) \tag{17}$$

To solve this equation, we must enumerate the two boundary conditions. Hence, we define a point $(x_S, y_S)$ near the sheath edge, where the condition of quasi-neutrality is still valid. Corresponding to this is the plasma solution given as:

$$Z_P\sqrt{\frac{b_{PS}+\sqrt{b_{PS}^2-4a_{PS}c_{PS}}}{2a_{PS}}}\cong Z_N\sqrt{\frac{-b_{NS}+\sqrt{b_{NS}^2-4a_{NS}c_{NS}}}{2a_{NS}}}+\exp\left(-y_S\right) \tag{18}$$

where $a_{PS}, b_{PS}, c_{PS}$ and $a_{NS}, b_{NS}, c_{NS}$ are defined above with the subscript '*S*' that designates the charged particle density at point $(x_S, y_S)$, obtained by setting $x = x_S$ and $y = y_S$ in Eq. (16). Another boundary condition is calculated by differentiating Eq. (18). This is stated as:

$$\left(\frac{dy}{dx}\right)_{\text{at S}}=\left[\begin{array}{l}-\frac{\sqrt{2a_{NS}}KM_Ni_N^2}{Z_Nx_s^{2K+1}M_P}\left(-b_{NS}+\sqrt{b_{NS}^2-4a_{NS}c_{NS}}\right)^{-\frac{1}{2}}\left(b_{NS}^2-4a_{NS}c_{NS}\right)^{-\frac{1}{2}}\\+\frac{\sqrt{2a_{PS}}Ki_P^2}{Z_Px_s^{2K+1}}\left(b_{PS}+\sqrt{b_{PS}^2-4a_{PS}c_{PS}}\right)^{-\frac{1}{2}}\left(b_{PS}^2-4a_{PS}c_{PS}\right)^{-\frac{1}{2}}\end{array}\right]$$
$$\times\left\{\begin{array}{l}\left[\frac{Z_N}{\sqrt{2a_{NS}}}\left(\frac{\left(-b_{NS}+\sqrt{b_{NS}^2-4a_{NS}c_{NS}}\right)^{-\frac{1}{2}}}{2}\right)\right]\left(-Z_N+Z_Nb_{NS}\left(b_{NS}^2-4a_{NS}c_{NS}\right)^{-\frac{1}{2}}\right)\\-\left[\frac{Z_P}{\sqrt{2a_{PS}}}\left(\frac{\left(b_{PS}+\sqrt{b_{PS}^2-4a_{PS}c_{PS}}\right)^{-\frac{1}{2}}}{2}\right)\right]\left(Z_P+Z_Pb_{PS}\left(b_{PS}^2-4a_{PS}c_{PS}\right)^{-\frac{1}{2}}\right)-\exp\left(-y_S\right)\end{array}\right\}^{-1} \tag{19}$$

Using these two boundary conditions [Eqs. (18)–(19)], we solve Poisson's equation numerically, defined in Eq. (17) for a particular set of parameters.

## Results and discussion

### Spherical geometry

For spherical geometry, geometric constant $K = 2$ and polytropic constant $C = 3$ are used. The behaviour of the electric potential is revealed by the Poisson's equation with the help of two appropriate boundary conditions which are described above [Eqs. (18)–(19)]. We have assigned a constant magnitude of the electric potential at the probe/wall surface (say $y_P \sim 100$) to determine the probe position, which in turn provided the information about the sheath thickness, i.e. $x_{PP} - x_S$. Here, $x_{PP}$ and $x_S$ correspond to the position of probe/wall and the sheath edge, respectively. The sheath thickness profile as a function of $T_P$ for different $T_N$ is portrayed herewith in Fig. 1 and observed noteworthy modifications. The impact of positive ions' temperature on the sheath thickness is important to study while dealing with surface–plasma interaction problems. This is because the temperature of positive ions imposed on the material surface may lead to significant modifications in its surface properties. The magnitude of the sheath thickness is enhanced with an increment in the $T_P$, whereas it is reduced with increased $T_N$. For lower $T_P$, the difference in the magnitude of the sheath thickness for different $T_N$ is minuscule; however, with increasing $T_P$, a significant difference in the magnitude of the sheath thickness is appeared for different $T_N$. For fixed $N_{N0}$, the density of the negative ions near the sheath edge is increased with an increased $T_N$. Therefore, the point where the condition of quasi-neutrality starts to hold is moved towards

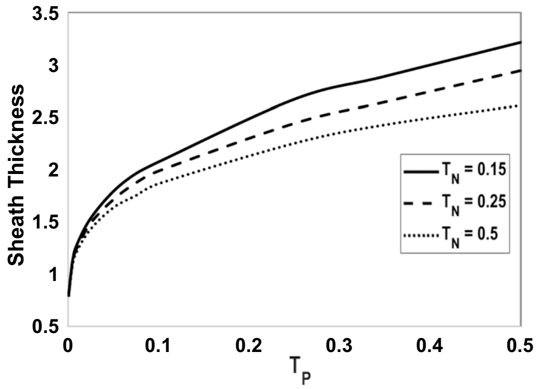


**Fig. 1** Sheath thickness profile as a function of $T_P$ for different $T_N$ when $K=2$, $Z_P=1$, $Z_N=1$, $M_P=69$, $M_N=19$, $N_{N0}=2$, $y_P=100$ and $x_P=10$

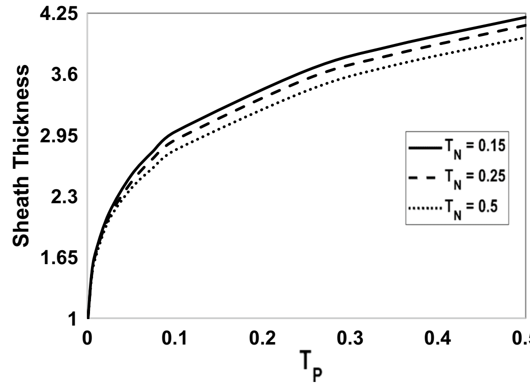


**Fig. 3** Sheath thickness profile as a function of $T_P$ for different $T_N$ when $K=1$, $Z_P=1$, $Z_N=1$, $M_P=69$, $M_N=19$, $N_{N0}=2$, $y_P=100$ and $x_P=10$

the probe/wall surface, which in turn results in a smaller sheath thickness.

The sheath thickness profile as a function of $N_{N0}$ for different $\frac{M_N}{M_P}$ is depicted in Fig. 2. We considered three electronegative plasmas: $CF_4$, $O_2$ and $C_{60}$. The majority of the positive and negative ions found in these plasmas are $CF_3^+$ and $F^-$, $O_2^+$ and $O^-$, $C_{60}^+$ and $C_{60}^-$, respectively. For these plasmas, the mass ratio of negative to positive ion turns to be 0.275, 0.5 and 1, respectively. The analysis of the mass ratio of negative to positive ions is imperative as it leads to considerable modifications in the profiles of the plasma parameters which will benefit in experimental applications such as plasma nitriding. The magnitude of the sheath thickness is enhanced with an increment in the $\frac{M_N}{M_P}$, whereas it is reduced with increased $N_{N0}$. For fixed $T_N$, a greater number of negative ions are available near the sheath edge with an enhanced $N_{N0}$. Consequently, a smaller sheath thickness is depicted for higher $N_{N0}$.

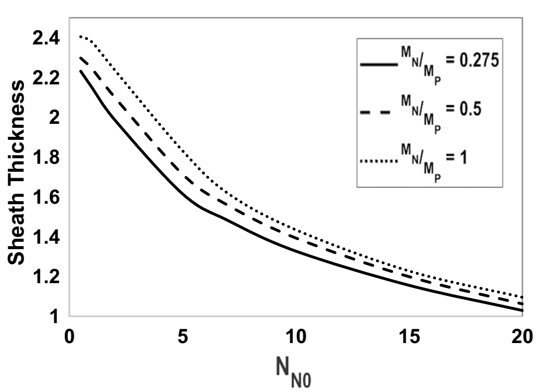


**Fig. 2** Sheath thickness profile as a function of $N_{N0}$ for different $\frac{M_N}{M_P}$ when $K=2$, $Z_P=1$, $Z_N=1$, $T_P=0.1$, $T_N=0.25$, $y_P=100$ and $x_P=10$

## Cylindrical geometry

For cylindrical geometry, geometry constant $K=1$ and polytropic constant $C=3$ are used. In Fig. 3, the magnitude of the sheath thickness as a function of $T_P$ for different $T_N$ is depicted. We found the magnitude of the sheath thickness to reduce with an increment in $T_N$, but to enhance with an increased $T_P$, consistent with the case of spherical geometry. However, for cylindrical geometry, the magnitude of the sheath thickness is relatively higher in comparison with the case of spherical geometry. In other words, for cylindrical geometry, shielding of the probe is not perfect; therefore, condition of quasi-neutrality occurs at a relatively larger distance from the probe/wall surface. The effect of positive (negative) ion temperatures on the sheath thickness remains the same in cylindrical geometry also, and the sheath thickness is increased (reduced) for higher temperature.

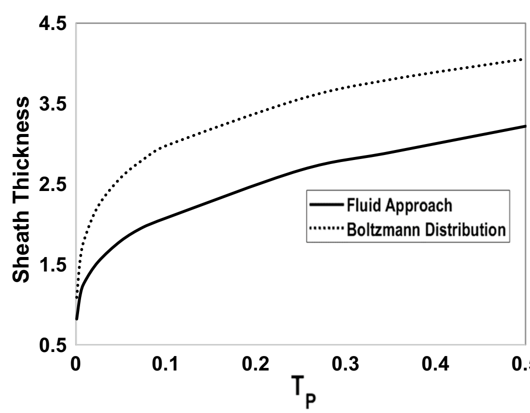


**Fig. 4** Comparative study of sheath thickness profile for the behaviour of negative ions by fluid approach and Boltzmann distribution as a function of $T_P$ when $K=2$, $Z_P=1$, $Z_N=1$, $M_P=69$, $M_N=19$, $N_{N0}=2$, $y_P=100$ and $x_P=10$, $T_N=0.15$

## Limiting cases

### Boltzmann distributed negative ions

A comparative study of the profile of the sheath thickness for the behaviour of the negative ions by Boltzmann distribution and fluid approach is entertained herewith and depicted in Fig. 4. The sheath of higher thickness is formed when negative ions obeyed Boltzmann distribution for all $T_P$. On comparing these two cases, for lower $T_P$, the difference in the magnitude of the sheath thickness is miniature, whereas a significant difference is obtained with increasing $T_P$. This difference is occurred due to the negligence of the mass of the negative ions and their drift term also. From this figure, it is clearly shown that drift term of the negative ions has a significant effect on the system; therefore, it should not be neglected.

### Electropositive plasma

The appropriate way to study the electropositive plasma using the same theoretical model is to omit out all the equations which described the behaviour of negative ions in the given system. In other words, we omit out the continuity and momentum transfer equation for the negative ions to investigate the sheath characteristics for a plasma without negative ions, i.e. for electropositive plasma. The resulting Poisson's equation is stated as follows:

$$\frac{\mathrm{d}^2 y}{\mathrm{d}x^2} + \frac{K}{x}\frac{\mathrm{d}y}{\mathrm{d}x} = \left( Z_P \sqrt{\frac{b_P + \sqrt{b_P^2 - 4a_P c_P}}{2a_P}} - \exp(-y) \right). \quad (20)$$

where $a_P = \frac{3T_P}{2} Z_P^2$, $b_P = \left( Z_P y + \frac{3T_P}{2} \right)$, and $c_P = \frac{i_P^2}{x^{2K} Z_P^2}$.

Corresponding to this [a point ($x_S$, $y_S$) near the sheath edge] is the plasma solution given as:

$$Z_P \sqrt{\frac{b_{PS} + \sqrt{b_{PS}^2 - 4a_{PS} c_{PS}}}{2a_{PS}}} \cong \exp(-y_S). \quad (21)$$

Another boundary condition is calculated by differentiating Eq. (21). This is stated as:

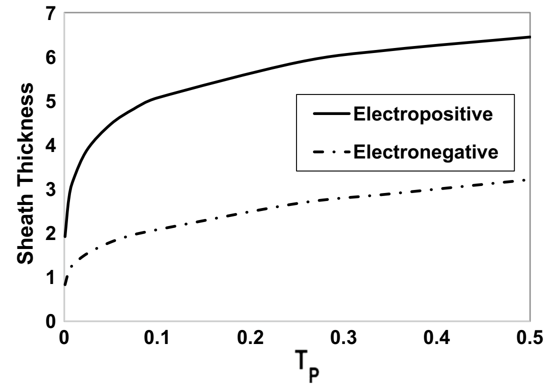


**Fig. 5** Comparative study of sheath thickness profile as a function of $T_P$ for electropositive and electronegative plasma when $K=2$, $Z_P=1$, $y_P=100$ and $x_P=10$ for electropositive plasma and $K=2$, $Z_P=1$, $Z_N=1$, $M_P=69$, $M_N=19$, $N_{N0}=2$, $T_N=0.15$, $y_P=100$ and $x_P=10$ for electronegative plasma

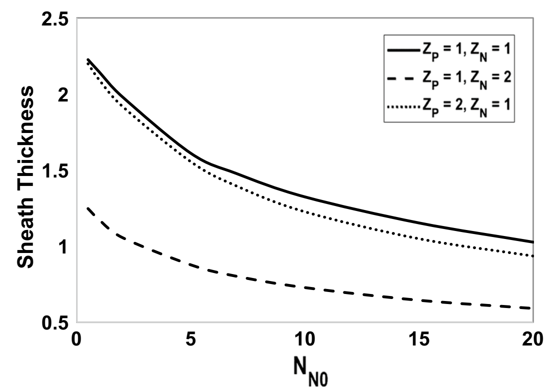


**Fig. 6** Comparative study of sheath thickness profile as a function of $N_{N0}$ for singly and doubly charged ions when $K=2$, $M_P=69$, $M_N=19$, $T_P=0.1$, $T_N=0.25$, $y_P=100$ and $x_P=10$

The comparative study of sheath thickness profile for electropositive and electronegative plasma is also entertained herewith and depicted in Fig. 5. The sheath thickness of higher magnitude is formed for electropositive plasmas for all cases of positive ions' temperature. The difference in the magnitude of the sheath thickness for these two cases increases with increasing positive ions' temperature.

$$\left(\frac{\mathrm{d}y}{\mathrm{d}x}\right)_{\text{at S}} = \left[ \frac{\sqrt{2a_{PS}} K i_P^2}{Z_P x_s^{2K+1}} \left( b_{PS} + \sqrt{b_{PS}^2 - 4a_{PS} c_{PS}} \right)^{-\frac{1}{2}} \left( b_{PS}^2 - 4a_{PS} c_{PS} \right)^{-\frac{1}{2}} \right] \times \left\{ - \left[ \frac{Z_P}{\sqrt{2a_{PS}}} \left( \frac{\left( b_{PS} + \sqrt{b_{PS}^2 - 4a_{PS} c_{PS}} \right)^{-\frac{1}{2}}}{2} \right) \right] \left( Z_P + Z_P b_{PS} \left( b_{PS}^2 - 4a_{PS} c_{PS} \right)^{-\frac{1}{2}} \right) - \exp(-y_S) \right\}^{-1}. \quad (22)$$

### Doubly charged ions

In most of the plasma systems, there is a finite concentration of the doubly charged ions. The concentration of such doubly charged ions depends upon the plasma parameters. The case of doubly charged ions in the plasma is investigated herewith and compared with the singly charged ions in Fig. 6. We have considered three cases: $Z_P = 1$ and $Z_N = 1$; $Z_P = 1$ and $Z_N = 2$; and $Z_P = 2$ and $Z_N = 1$. From Fig. 6, we have observed a significant modification in the magnitude of the sheath thickness when negative ions are doubly charged, whereas a minuscule modification in the magnitude of the sheath thickness is detected when positive ions are doubly charged.

The advantage of adopting spherical and cylindrical probes in the plasma processing is the production of large saturation current for the same density, which, in turn, plays a momentous advantage for measurements in the regions of very low density.

## Conclusions

We studied the effect of negative to positive ion mass ratio for the very first time for different plasma conditions to understand the exact sheath behaviour. The magnitude of the sheath thickness is found to be larger when the mass ratio is larger, and the positive ions carry higher temperature, whereas negative ions carry lower temperature. Sheath behaviour is strongly depending on the electronegativity of the medium, and its thickness is reduced with an increment in the electronegativity. A comparative study of cylindrical and spherical probes yields that the sheath of higher magnitudes is formed in cylindrical case. Additionally, the results for fluid behaviour of negative ions are compared with Boltzmann distribution of negative ions to have a better understanding of the problem proposed here. It is depicted that the sheath of lower magnitude is resulted for the case of fluid approach. This difference is arisen due to the negligence of the drift term. This noteworthy difference between the two cases justified the worth consideration of the drift term of negative ions and the mass of the negative ions. These results shall play an imperative role in those experimental fields where the plasmas composed of negative ions are preferred and also where the temperature of ions has a considerable effect on the surface properties. The investigation of doubly charged ions is also conducted and observed a significant reduction in the magnitude of the sheath thickness when negative ions are doubly charged in comparison with singly charged negative ions.

**Acknowledgements** Rajat Dhawan acknowledges the Council of Scientific and Industrial Research, Govt. of India, for providing the financial support [Grant Reference Number: 09/086(1289)/2017-EMR-1].

## References


1. Shibata, K., Nishida, Y., Yugami, N.: Production of thin-film by sheet-shaped plasma. Mater. Inst. Electr. Eng. PST, Plasma Soc. **1997**, 59–62 (1997)
2. Shibata, K., Ito, H., Yugami, N., Miyazaki, T., Nishida, Y.: Production of Nb thin film by ECR sheet plasma. Thin Solid Films **386**, 291–294 (2001)
3. Lieberman, M.A., Lichtenberg, A.J.: Principles of Plasma Discharges And Materials Processing. Wiley, London (2005)
4. Hatada, R., Flege, S., Bobrich, A., Ensinger, W., Baba, K.: Surface modification and corrosion properties of implanted and DLC coated stainless steel by plasma based ion implantation and deposition. Surf. Coat. Technol. **256**, 23–29 (2014)
5. Kostov, K.G., Machida, M., Prysiazhnyi, V., Honda, R.Y.: Transfer of a cold atmospheric pressure plasma jet through a long flexible plastic tube. Plasma Sources Sci. Technol. **24**, 25038 (2015)
6. Dorranian, D., Abedini, Z., Hojabri, A., Ghoranneviss, M.: Structural and optical characterization of PMMA surface treated in low power nitrogen and oxygen RF plasmas. J. Non-Oxide Glasses **1**, 217–229 (2009)
7. Jafari, M., Dorranian, D.: Surface modification of PMMA polymer in the interaction with oxygen-argon RF plasma. J. Theor. Appl. Phys. **5**, 59–66 (2011)
8. Singh, O., Malik, H.K., Dahiya, R.P., Kumar, P.: Influence of negative bias voltage on structural and mechanical properties of nanocrystalline TiNx thin films treated in hot cathode arc discharge plasma system. Ceram. Int. **42**, 18019–18024 (2016)
9. Singh, O., Dahiya, P., Malik, H.K., Kumar, P., Singh, V.: Investigation of titanium nitride thin films treated in hot cathode arc discharge plasma system. Appl. Sci. Lett. **2**, 37–41 (2016)
10. Dhawan, R., Malik, H.K.: Theoretical study of plasma-material interaction. AIP Conf. Proc. **2162**, 20136 (2019)
11. Abe, H., Yoneda, M., Fujiwara, N.: Developments of plasma etching technology for fabricating semiconductor devices. Jpn. J. Appl. Phys. **47**, 1435–1455 (2008)
12. Makabe, T., Petrovic, Z.L.: Plasma Electronics: Applications in Microelectronic Device Fabrication. CRC Press, Boca Raton (2014)
13. Aanesland, A., Bredin, J., Chabert, P.: A review on ion–ion plasmas created in weakly magnetized electronegative plasmas. Plasma Sources Sci. Technol. **23**, 44003 (2014)
14. Buuron, A., Koch, F., Nöthe, M., Bolt, H.: Diagnostics and modeling of a hollow-cathode arc deposition plasma. Surf. Coat. Technol. **116**, 755–765 (1999)
15. Blawert, C., Weisheit, A., Mordike, B.L., Knoop, R.M.: Plasma immersion ion implantation of stainless steel: austenitic stainless steel in comparison to austenitic–ferritic stainless steel. Surf. Coat. Technol. **85**, 15–27 (1996)
16. Kennedy, R.V., Allen, J.E.: The floating potential of spherical probes and dust grains. Part 1. Radial motion theory. J. Plasma Phys. **67**, 243–250 (2002)
17. Kennedy, R.V., Allen, J.E.: The floating potential of spherical probes and dust grains. II: Orbital motion theory. J. Plasma Phys. **69**, 485–506 (2003)
18. Starodubtsev, M., Kamal-Al-Hassan, M., Ito, H., Yugami, N., Nishida, Y.: Low-frequency sheath instability in a non-Maxwellian plasma with energetic ions. Phys. Rev. Lett. **92**, 45003 (2004)

19. Kamal-Al-Hassan, M., Starodubtsev, M., Ito, H., Yugami, N., Nishida, Y.: Observation of ion wave streamers and low frequency sheath instability by the resonant absorption due to nonlinear interaction of microwave-plasma. Phys. Plasmas **11**, 836–843 (2004)
20. Starodubtsev, M., Kamal-Al-Hassan, M., Ito, H., Yugami, N., Nishida, Y.: Low-frequency sheath instability stimulated by an energetic ion component. Phys. Plasmas **13**, 12103 (2006)
21. Atalay, B., Aydin, R., Demir, A., Kenar, N., Kacar, E.: Simulation of Ni-like and Co-like X-rays emitted from laser produced tin plasmas. Czechoslov. J. Phys. **56**, B430–B435 (2006)
22. Demir, P., Kacar, E., Akman, E., Bilikmen, S.K., Demir, A.: Theoretical and experimental investigation of soft X-rays emitted from TIN plasmas for lithographic application. In: Ultrafast X-Ray Sources and Detectors, p. 67030B. International Society for Optics and Photonics (2007)
23. Demir, P., Kacar, E., Bilikmen, S.K.: Demir A (2009) Conversion efficiency calculations for soft X-rays emitted from tin plasma for lithography applications. In: Lewis, C.L.S., Riley, D. (eds.) X-Ray Lasers, pp. 281–287. Springer, Dordrecht (2009)
24. Araghi, F., Dorranian, D.: Effect of negative ions on the characteristics of plasma in a cylindrical discharge. J. Theor. Appl. Phys. **7**, 41 (2013)
25. Dorranian, D., Alizadeh, M.: Effect of negative oxygen ions on the characteristics of plasma in a cylindrical DC discharge. J. Theor. Appl. Phys. **8**, 122 (2014)
26. Proshina, O.V., Rakhimova, T.V., Rakhimov, A.T., Voloshin, D.G.: Two modes of capacitively coupled rf discharge in CF4. Plasma Sources Sci. Technol. **19**, 65013 (2010)
27. Berezhnoj, S.V., Shin, C.B., Buddemeier, U., Kaganovich, I.: Charged species profiles in oxygen plasma. Appl. Phys. Lett. **77**, 800–802 (2000)
28. Sato, N., Mieno, T., Hirata, T., Yagi, Y., Hatakeyama, R., Iizuka, S.: Production of C60 plasma. Phys. Plasmas **1**, 3480–3484 (1994)
29. Oohara, W., Hatakeyama, R.: Pair-ion plasma generation using fullerenes. Phys. Rev. Lett. **91**, 205005 (2003)
30. Kono, A.: Formation of an oscillatory potential structure at the plasma boundary in electronegative plasmas. J. Phys. D Appl. Phys. **32**, 1357 (1999)
31. Sheridan, T.E., Chabert, P., Boswell, R.W.: Positive ion flux from a low-pressure electronegative discharge. Plasma Sources Sci. Technol. **8**, 457 (1999)
32. Kono, A.: Complex sheath formation around a spherical electrode in electronegative plasmas: a comparison between a fluid model and a particle simulation. J. Phys. D Appl. Phys. **34**, 1083 (2001)
33. Ping, D., Zhengxiong, W., Wenchun, W., Jinyuan, L., Yue, L., Xiaogang, W.: Sheath structures of strongly electronegative plasmas. Plasma Sci. Technol **7**, 2649 (2005)
34. Sharifian, M., Shokri, B.: Behavior of the floating potential in an electronegative sheath as a function of electronegativity and negative ion temperature. J. Plasma Phys. **77**, 307–314 (2011)
35. Regodón, G.F., Palop, J.I.F., Tejero-del-Caz, A., Díaz-Cabrera, J.M., Carmona-Cabezas, R., Ballesteros, J.: Floating potential in electronegative plasmas for non-zero ion temperatures. Plasma Sources Sci. Technol. **27**, 25014 (2018)

**Publisher's Note** Springer Nature remains neutral with regard to jurisdictional claims in published maps and institutional affiliations.